Proceedings of 2005 5th IEEE Conference on Nanotechnology
Nagoya, Japan, July 2005

# Characterization of 2D-Photonic Crystal Nanocavities by Polarization-Dependent Photoluminescence

Y. Tang, [1,*] A. M. Mintairov, [1] J. L. Merz, [1] V. Tokranov[2] and S. Oktyabrsky[2]

[1]Dept. Electrical Engineering, University of Notre Dame, Notre Dame IN 46556
[2]Institute for Materials, State University of New York at Albany, Albany NY 12203

***Abstract* — In this work, hexagonal defect nanocavities ("*H1*" and "*H2*") in two-dimensional photonic crystal slabs were fabricated in a half wavelength-thick semiconductor waveguide embedded with quantum dots. We characterized the cavity modes with polarization sensitive micro-photoluminescence. The polarization property of the spontaneous emission was shown to be an effective approach for detecting the symmetry of the modes, from which the mode structure for an *H2*-cavity was experimentally verified for the first time.**

***Index Terms* — Nanocavity, photonic crystals, semiconductor quantum dots.**

## I. Introduction

Semiconductor thin film-based photonic crystals (PC) have attracted much attention as potential experimental systems for cavity-quantum electrodynamics due to their extremely small mode-volume and the controllability of the electromagnetic field inside the PC nanocavity, in combination with the availability of atom-like emission from individual quantum dots (QDs). Theoretical cavity modes with specific frequencies, patterns and polarization properties can be achieved via proper design [1,2]. However, inevitable errors during fabrication would bring imperfection into real devices, which breaks the symmetry of the cavity and changes aspects of certain modes.

In this work, we studied the in-plane polarization properties of resonant modes of the single-defect cavity (*H1*) and the seven-defect cavity (*H2*) formed in a 2D-hexagonal lattice of air holes in a semiconductor slab waveguide. The mode structure was probed with the broadband emission from an ensemble of self-assembled InAs QDs and characterized with polarization sensitive micro-photoluminescence ($\mu$PL).

In the *H1*-cavity, a pair of dipole modes with $E_1$ symmetry [3] dominates the QDs' emission. Though these two modes should be degenerate in a perfect hexagonal lattice with six-fold symmetry ($C_{6v}$), they split into two orthogonally polarized modes as a consequence of reduced symmetry from $C_{6v}$ to $C_{2v}$ by lattice distortion. The lattice distortion was analyzed by 2D-fast Fourier transform (FFT) and then applied to the simulation. The calculated frequency and polarization associated with each mode agree well with the $\mu$PL experiments. The *H2*-cavity, formed by removing seven adjacent air-holes at the center of the lattice, has a much larger mode volume than the *H1*-cavity. Within the emission band of QDs there exist both non-degenerate and doubly-degenerate modes, which possess six-fold symmetry ($A_1$, $A_2$ or $B_2$) and two-fold symmetry ($E_1$), respectively. From the specific polarization properties exhibited by each mode, we made the first experimental verification of the mode structure of the *H2*-cavity, which is entirely consistent with the theoretical simulation.

## II. Cavity design

The photonic band structure of a hexagonal lattice PC slab and *H1*-cavity modes were modeled using the 3D block-iterative frequency-domain method [4], as shown in Fig.1. The band gap for TE (TM)-like guided modes as a function of air-hole radius *r* (normalized with lattice period *a*) is plotted as the light gray area between two thick (thin) solid lines. In this case TE-like modes are of most interest because of a much wider band gap. Two pairs of doubly degenerate (*x*,*y*)-dipole modes (*E1*) having energies within the lowest TE-gap, are well confined in the *H1*-cavity (Fig.1, dots and squares). The electric field energy distributions of these modes at the center plane of the PC slab are presented in the insets to Fig.1.

## III. Experimental Details

### *A. Fabrication Procedure*

The PC nanocavities were fabricated on a GaAs-$Al_xGa_{1-x}As$ heterostructure grown on (100) GaAs substrate by molecule beam epitaxy, It consists of 500nm $Al_{0.95}Ga_{0.05}As$ as sacrificial layer and a waveguide layer on top of it which is composed of 170nm-thick GaAs sandwiched between two 40nm-thick $Al_{0.3}Ga_{0.7}As$ layers and two 5nm-thick GaAs layers successively. A single layer of self-assembled InAs QDs with a dot density of about $5\times10^{10}cm^{-2}$ was inserted in the center of the wave-

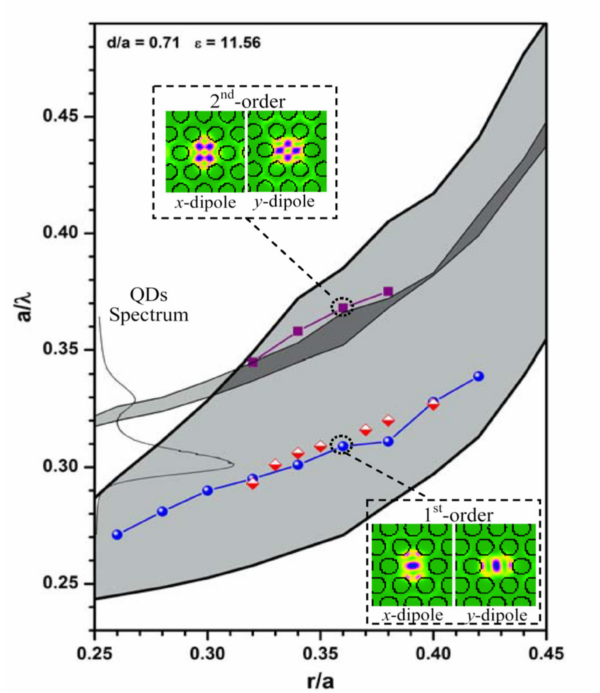


Fig.1. Photonic band structure of 2D hexagonal lattice PC slab and H1-cavity modes as functions of air-hole radius. The slab thickness d = 0.71a. Light gray area between two thick (thin) solid lines is the first band gap for TE (TM)-like guided modes. Dark gray area is band gap for both polarizations. Dots and squares represent frequencies of 1st- and 2nd-order dipole mode, respectively. Diamonds represent experimental data. Insets show the electric field intensity profile of the modes.

guide layer, to provide a broad-band emitter working at room temperature. The energy spectrum of the QDs' emission is compared with the band structure of the PC in Fig.1 to seek optimized lattice parameters for coupling. A set of PC cavity patterns with lattice constant *a* of 366nm and variable air-holes radii from 0.3*a* to 0.4*a* were first generated with electron-beam lithography into 950K PMMA e-beam resist and then transferred through the waveguide region via $BCl_3$/Ar reactive ion etching. The free-standing slab waveguides were finally realized by selectively wet etching the $Al_{0.95}Ga_{0.05}As$ sacrificial layer beneath the waveguide with diluted HF acid. The scanning electron micrograph (SEM) images of *H1* and *H2* cavities with *r/a* ratio of 0.37 is shown in Fig.2.

*B. Optical Measurements*

Optical measurements in this work were carried out at room temperature. The sample was mounted on a three-dimensional adjustable stage. The PC defect cavities are optically pumped with an Ar-ion laser at a wavelength of

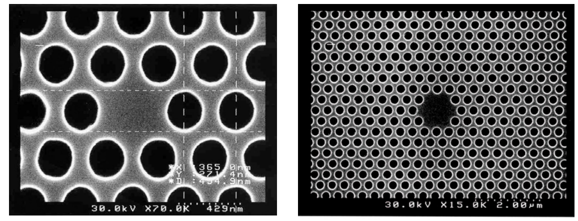


Fig. 2. Scanning electron micrograph image of *H1* and *H2* PC defect cavities

514.5nm. The laser was vertically focused on the cavity region through an 80X microscope objective, resulting in a power density of about $500W/cm^2$. The same objective was also used to image the sample and to collect the PL emitted from the sample surface. The collected PL signal was then dispersed with a 0.5m spectrometer and recorded with a liquid-nitrogen cooled InGaAs CCD detector. The spatial resolution of this micro-PL setup is about 2μm with the use of a 200μm confocal pinhole.

For the polarization experiment, a linear polarizer was placed in the beam path after the collection lens, which filters the different in-plane polarization components of the collected $\mu$PL.

## IV. Results and Discussion

*A. H1-cavity*

The $\mu$PL spectra from *H1*-cavities with variable air-hole radii are displayed in Fig.3. For comparison, the PL spectrum of an unprocessed MBE-grown QD sample is also plotted. The two Gaussian-like emission bands from the reference sample, centered at 1210nm and 1110nm respectively, are recombination of the ground state and first excited state electron-hole pairs in the QDs. The width of each band reflects the size fluctuation of the self-assembled QDs. In contrast to the broad emission bands from the QD-ensemble, the $\mu$PL from the *H1*-cavities shows sharp lines sweeping across the QD emission band with increasing *r/a* ratio, with significant enhancement of spontaneous emission of the QDs. The line width of the modes is limited by the quality factor of the cavity (Q~200-300). The mode intensity gets stronger when the cavity modes come into resonance with the majority of the QDs, i.e. close to the peak position of the Gaussian-like band. The center resonant frequency of each cavity (Fig.1, half-filled diamonds) fits well with the theoretical expectation for a 1st-order dipole-like mode, though the splitting was not expected from the simulation.

Meanwhile we can see a distinct splitting of the double

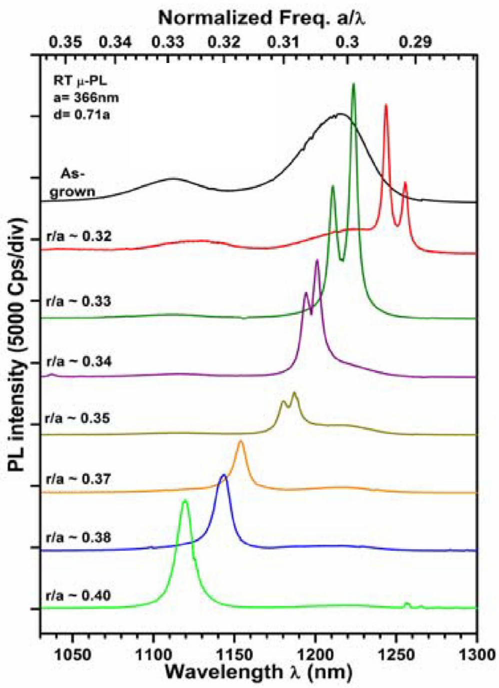


Fig. 3. RT micro-PL spectra of H1-cavities with different air-hole radii. The as-grown QD luminescence (ensemble of QDs) is the top spectrum.

degeneracy in some of the fabricated cavities. We ascribe such splitting to lattice distortion, most likely introduced during electron-beam lithography. For verification, the polarization of the mode was inspected for the *H1*-cavity with r/a ratio of 0.32. As can be seen in Fig.4(a), the two branches of the cavity mode are polarized along *x*- and *y*-directions, respectively. The lower frequency associated with *x*-polarization implies the PC lattice is either elongated along the *y*-direction or compressed along the *x*-direction. This was confirmed through 2D-FFT of the SEM of the whole hexagonal lattice. The reciprocal lattice vector along the y-direction is found to be 3% smaller than that along the other two equivalent axial directions, which means in the real lattice, the period in the *x*-direction should be about 3% larger than in the other two equivalent axial directions, Considering this distortion in the simulation, we calculated resonant frequencies of *x*- and *y*-dipole modes at 0.291 and 0.294 respectively, in good agreement with the measured x- and y-polarized modes at 0.292 and 0.294 in the PL spectrum.

*B. H2-cavity*

The micro-PL spectrum from an *H2*-cavity with *r/a* ratio of 0.37 and its polarization dependence are presented

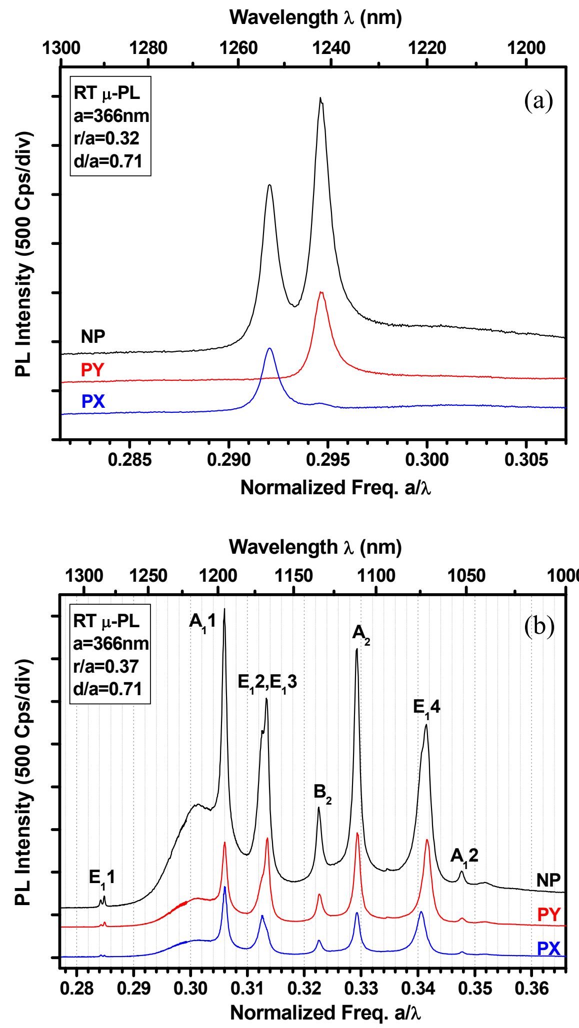


Fig. 4. Polarization-dependence of PL spectra of the *H1*-cavity (a) and *H2*-cavity (b) at room temperature. For each cavity the spectrum was taken without polarizer (NP), and with the polarizer oriented along the *x* or *y*-direction (PX or PY).

in Fig.4(b). Unlike the situation for an *H1*-cavity, the spectrum shows the presence of multiple resonance peaks within the emission range of the QDs, due to the much larger defect size. For the modes with frequencies centered at 0.285, 0.312, 0.313 and 0.341, the *x*-polarized components shift about 0.01 to the lower frequency side with respect to the *y*-polarized components, which indicates these modes have double-degeneracy and the imperfection of the cavity causes a frequency-shift between the *x*- and *y*-polarized components. For the other modes with frequencies centered at 0.306, 0.323, 0.329 and 0.348, not only is the line width of each mode about

TABLE I *H2*-cavity modes

| **Non-degenerate Modes** | | | | | **Doubly-degenerate Modes** | | | | |
|---|---|---|---|---|---|---|---|---|---|
| Mode | | Normalized freq. a/ λ | | E-field intensity profile | Mode | | Normalized freq. a/ λ | | E-field intensity profile |
| | | Measured | Simulated | | | | Measured | Simulated | |
| $A_1$ | 1 | 0.306 | 0.304 | 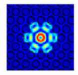 | $E_1$ | 1 | 0.285 | 0.283 | 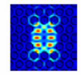 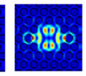 |
| $A_1$ | 2 | 0.348 | 0.352 | 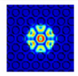 | $E_1$ | 2 | 0.312 | 0.312 | 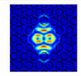 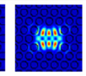 |
| $A_2$ | | 0.329 | 0.332 | 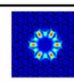 | $E_1$ | 3 | 0.313 | 0.313 | 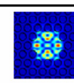 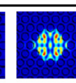 |
| $B_2$ | | 0.323 | 0.323 | 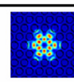 | $E_1$ | 4 | 0.341 | 0.349 | 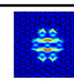 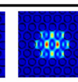 |

half of the above modes, but also there is no shift in frequency between its *x*- and *y*-polarized components, which is a sign that these modes are non-degenerate.

The mode structure of the *H2*-cavity was simulated and matched with the measured mode frequencies in TABLE 1. We also denoted each resonance peak in Fig.4(b) with its corresponding symmetry. As expected, the doubly-degenerate modes ($E_1$*1-4)* are dipole-like, though the electric-field intensity distribution is more complicated than in *H1*-cavity. The four non-degenerate modes belong to three different symmetry groups, which include the monopole-like modes ($A_1$*1,2)*, the whispering-gallery-mode ($A_2$) and the hexapole-like mode ($B_2$). Both the mode frequency and characteristic polarization associated with each mode obtained from the micro-PL experiment correspond well with the simulated results.

We are currently employing near-field scanning optical microscopy (NSOM) to characterize the E-field intensity of the modes in the *H2-cavity* and have obtained preliminary results [5]. Work is in progress to improve the resolution of the scans, and to compare them with calculated modes.

## V. Conclusion

We successfully designed and fabricated 2D hexagonal PC defect cavities ("*H1*" and "*H2*") based on a GaAs-$Al_xGa_{1-x}As$ waveguide structure containing InAs QDs. The resonant modes of these cavities were characterized with polarization-dependent micro-PL. It has been shown that because of the imperfection in the fabrication process, and consequent lowering of the symmetry of the PC lattices, the doubly-degenerate dipole-like modes in both the *H1* and *H2* cavities will split into two orthogonally polarized modes, while the non-degenerate modes (in the *H2-cavity*) show no sign of splitting. Based on the different polarization properties of each mode, we achieved very good agreement between the simulated and measured mode structure of an H2-cavity.

## Acknowledgement

The support of the W.M. Keck Foundation and the University of Virginia NSF MRSEC are gratefully acknowledged.

## References

[1] O. Painter, K. Srinivasan, J. D. O'Brien, A. Sherer and P. D. Dapkus, "Tailoring of the resonant mode properties of optical nanocavities in two-dimensional photonic crystal slab waveguides," *J. Opt. A*, Vol. 3, No. 6, S161-S170, November 2001.

[2] O. Painter and K. Srinivasan, "Polarization properties of dipolelike defect modes in photonic crystal nano-cavities", Opt. Lett., Vol. 27, No. 5, pp 339-341, March 2002.

[3] K. Sakoda, *Optical Properties of Photonic Crystals,* Springer 2001.

[4] S. G. Johnson and J. D. Joannopoulos, "Block-iterative frequency-domain methods for Maxwell's equations in a planewave basis", *Opt. Express*, Vol. 8, No.3, pp 173 - 190, January 2001.

[5] A. M. Mintairov, Y. Tang, J. L. Merz, V. Tokranov, and S. Oktyabrsky, "Single dot near-field spectro-scopy for photonic crystal microcavities", phys. stat. sol. Vol. c **2**, pp 845 – 849, 2005.

* Present address: 104 Davey Laboratory, Penn State University, State Colleg e, PA 16802